A new analysing approach for the structure of density fluctuation of supercritical fluid

2008 J. Phys.: Condens. Matter 20 104203

(http://iopscience.iop.org/0953-8984/20/10/104203)

J. Phys.: Condens. Matter **20** (2008) 104203 (6pp) doi:10.1088/0953-8984/20/10/104203

A new analysing approach for the structure of density fluctuation of supercritical fluid

T Sato[1], M Sugiyama[1,4], M Misawa[2], S Takata[3], T Otomo[2], K Itoh[1], K Mori[1] and T Fukunaga[1]

[1] Research Reactor Institute, Kyoto University, Osaka 590-0494, Japan
[2] High Energy Accelerator Research Organization, Ibaraki 305-0801, Japan
[3] Japan Atomic Energy Agency, Tokai, Ibaraki 319-1195, Japan

E-mail: sugiyama@rri.kyoto-u.ac.jp

Received 5 November 2007, in final form 28 December 2007
Published 19 February 2008
Online at stacks.iop.org/JPhysCM/20/104203

Abstract

Large scale structural evolution of supercritical carbon dioxide along the isotherm at 32 °C was investigated with small-angle neutron scattering. The maximum of the density fluctuation, the so-called 'ridge', was confirmed with Ornstein–Zernike analysis. To investigate the structural change in more detail, the molecular distribution over a large domain was determined with a newly developed reverse Monte Carlo method. From the molecular distribution obtained, the pair distribution function and cluster-size distribution can be calculated. With increasing density of carbon dioxide, the cluster size increases monotonically, whereas the pair distribution function for the range of sizes shorter than 10 Å shows a monotonic decrease. From this result, it is suggested that the structural change along the isotherm is caused by the change of balance between growth of clusters and increase of the average density.

1. Introduction

Recently, supercritical carbon dioxide (sc-CO_2) has been recognized as an environmentally acceptable solvent for reaction chemistry. The solubility of sc-CO_2 can be easily controlled with a small change of its thermodynamic state. This solvent property is strongly connected with the structure of density fluctuation of CO_2 molecules. In particular, the solubility drastically changes when the density fluctuation becomes maximum in the supercritical region, the so-called 'ridge' [1–5]. Therefore, clarification of the large scale structural change over the ridge is quite important not only for understanding the origin of its solubility but also for developing new applications of sc-CO_2.

In the last 15 years, many researchers have vigorously studied the structure of sc-CO_2 with scattering experiments and computer simulations [1–11]. Although the studies of the local structure have succeeded in revealing orientational correlation between CO_2 molecules precisely, the large scale structures, such as the density fluctuation, the formation of molecular clusters and so on, have been less understood. To investigate the large scale structure, the molecular distribution over a large domain is essential information because the size of molecular clusters and the strength of the pair correlation can be easily obtained with the distribution. However, it has been difficult to obtain the molecular distribution over a large domain with previous methods. For example, with the computational calculation using an intermolecular potential model, the distribution cannot be obtained within a reasonable time. On the other hand, experimental methods, such as small-angle neutron and x-ray scattering (SANS and SAXS) ones, give us information on large scale structure. However, the information is not a molecular distribution but only some statistical parameters, e.g. the fluctuation of the number density $((\langle n^2\rangle - \langle n\rangle^2)/\langle n\rangle$; n: number of molecules in the corresponding volume V) and the Ornstein–Zernike correlation length. Therefore, a new analysing method which can derive the molecular distribution from the scattering data is necessary for understanding the large scale structure. For this purpose, we have focused on a reverse Monte Carlo (RMC) method [12]. Although only a few applications of the RMC method to SANS have been reported [13], this method shows

[4] Author to whom any correspondence should be addressed.

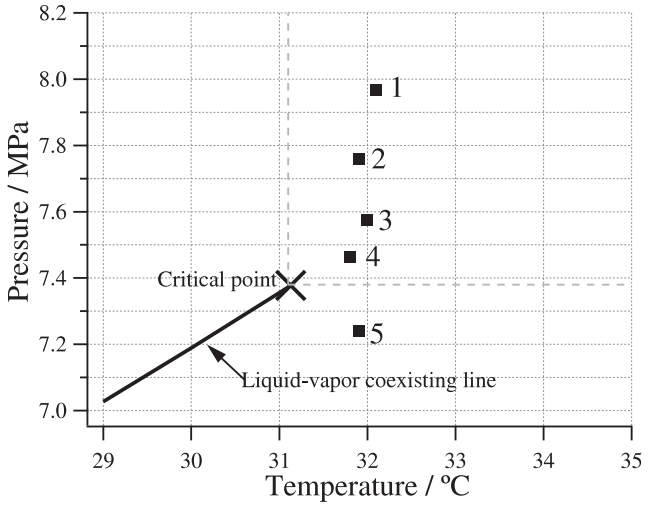

Figure 1. Thermodynamic states of sc-CO_2 observed in this study. The numbers 1–5 indicate each of the measurement points listed in table 1.

Table 1. Thermodynamic states of sc-CO_2 in the SANS experiment and calculating conditions for the RMC method. T, P, and ρ are temperature, pressure, and density, respectively. ξ is the Ornstein–Zernike correlation length. N is the number of molecules used in the RMC calculation. C.P. indicates a critical point of CO_2.

State	T (°C)	P (MPa)	ρ (g cm^{-3})	ξ (Å)	N
C.P.	31.1	7.38	0.468	—	—
1	32.1	7.97	0.645	12.9	176 115
2	31.9	7.76	0.620	16.2	168 869
3	32.0	7.57	0.538	42.1	146 843
4	31.8	7.46	0.362	20.5	98 779
5	31.9	7.24	0.279	11.1	76 030

the possibility of finding the molecular distribution over a large domain without any potential model.

In this study, the SANS intensity of sc-CO_2 along the isotherm at 32 °C was measured in order to reveal the structural change over the ridge. Since this temperature is quite close to the critical temperature (31.1 °C), the structural change is expected to be significant around the ridge. In addition, we have developed a new RMC method for the SANS analysis and determined the distribution of all CO_2 molecules on a large scale. With the results of RMC analysis, the origin of the ridge has been discussed.

2. Experimental procedure

SANS experiments on sc-CO_2 (the purity is 99.99%) were carried out by using a time-of-flight small/wide-angle neutron scattering instrument (SWAN) [14] installed at the High Energy Accelerator Research Organization (KEK) in Tsukuba, Japan. SANS intensities were measured at five thermodynamic states (states 1–5) along the isotherm on 32 °C displayed on a phase diagram (figure 1). The thermodynamic parameters for each state are listed in table 1.

A pressure cell was made of SUS316 with two sapphire windows. Temperature and pressure were measured by a

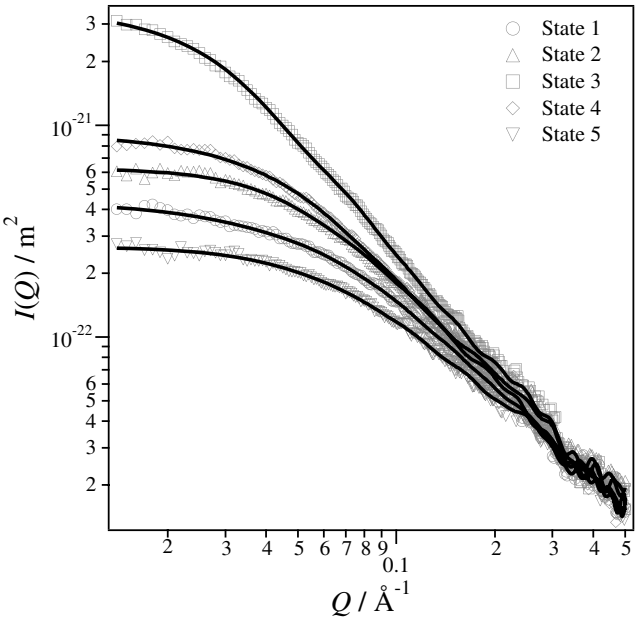

Figure 2. SANS intensities for sc-CO_2 at states 1–5 (table 1). Solid curves show the results of RMC calculation.

T-type thermocouple and a pressure sensor (Tem. Tech. Lab. NPS 3200BOX-1MW), respectively. The temperature was controlled by circulating water through a jacket of the pressure cell. During the measurement, deviations of temperature and pressure were kept within ±0.2 °C and ±0.03 MPa, respectively [15]. In the following analysis, SANS data between $Q = 0.01$ Å^{-1} and 0.5 Å^{-1} (Q: the magnitude of the scattering vector) were used.

3. Result of the SANS experiment

Figure 2 shows the SANS intensities at states 1–5. The scattering intensities in the low Q range are monotonically increasing from state 1 to state 3, while they are decreasing from state 3 to state 5. This means that the density fluctuation becomes maximum around state 3. To evaluate this change quantitatively, the Ornstein–Zernike correlation length, ξ, was calculated with the following equation:

$$I(Q) = \frac{I(0)}{1 + \xi^2 Q^2}, \tag{1}$$

where $I(0)$ is the scattering intensity at $Q = 0$. The so-called Ornstein–Zernike plots of $I(0)/I(Q)$ versus Q^2 are shown in figure 3. The correlation lengths at all states obtained from the slope of Ornstein–Zernike plot are also listed in table 1 and their density dependence is shown in figure 4. As expected, the correlation length drastically changes around state 3 on this isotherm: the maximum of the correlation length along the isotherm, i.e. the 'ridge', can obviously be confirmed. In addition, it is worth noting that this is the first direct observation of the 'ridge' with such large fluctuation.

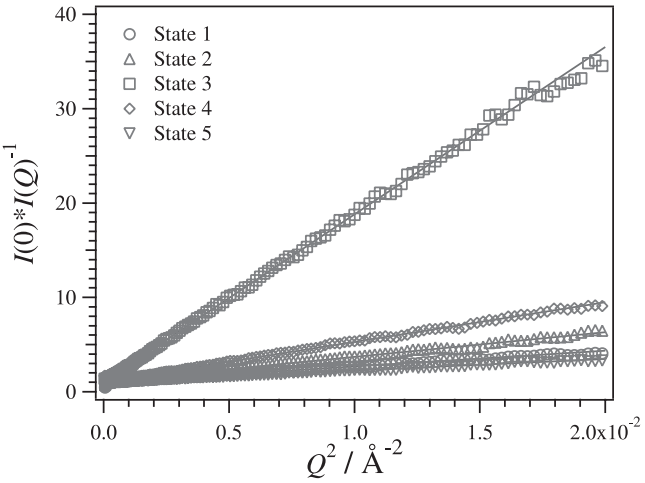

Figure 3. Ornstein–Zernike plots for SANS data. The solid lines indicate the results of the analysis with the Ornstein–Zernike equation.

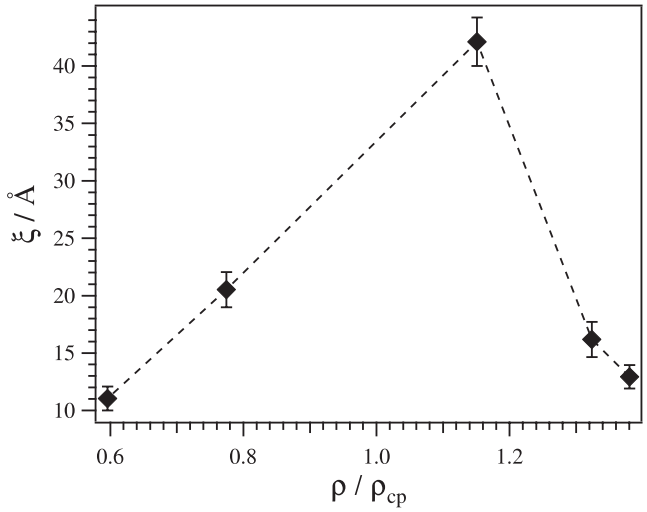

Figure 4. Density dependence of the correlation length, ξ. The existence of the maximum, the ridge, can be clearly confirmed.

4. Reverse Monte Carlo analysis

In order to investigate the large scale structure in detail, the molecular distribution on a large scale should be clarified. Therefore, we have developed a new RMC method for deriving the molecular distribution from the SANS spectra. In this section, we describe the detail of the RMC method developed and the results of applying it to the observed SANS data.

4.1. Development of the RMC method

A large domain is required for the calculation in order to reveal the structure of the density fluctuation consisting of a lot of CO_2 molecules. The size of domain was determined with the following procedure. First, the characteristic length of a CO_2 molecule, a, is estimated to be 3.39 Å by using an equation for the critical packing fraction [16, 17]:

$$\frac{\pi}{6}\rho_{\mathrm{cp}}a^3 = 0.130\,44, \tag{2}$$

where ρ_{cp} (=6.40 × 10^{-3} Å^{-3}) is the number density of CO_2 molecules at the critical point. The length a completely corresponds to the intermolecular distance observed in previous studies [5–9]. Next, the volume of the computational domain was chosen to be $(271.2)^3$ Å^3 with 80 × 80 × 80 grids of the length a. The validity of this size will be discussed in section 4.2.

As an initial distribution, CO_2 molecules were randomly put on the grid points with an allowed deviation of $\pm 0.3a$. The scattering intensity $I(Q)$ from the computational domain is calculated from

$$I(Q) = Nf(Q)\left\{1 + \int 4\pi r^2 \rho_{\mathrm{CO_2}}\,(g(r) - 1)\,\frac{\sin Qr}{Qr}\,\mathrm{d}r\right\}, \tag{3}$$

where N is the number of molecules in the domain listed in table 1 which is derived from the equation of state for CO_2 [18]. $f(Q)$, $g(r)$, and $\rho_{\mathrm{CO_2}}$ are an isotropic form factor of a CO_2 molecule, a pair distribution function of CO_2 molecules, and the number density of the system, respectively. A reliability factor, χ, which indicates the difference between the observed intensity, $I_{\mathrm{exp}}(Q)$, and the calculated one, $I_{\mathrm{calc}}(Q)$, is defined as follows;

$$\chi = \sqrt{\sum_{i=1}^{n}\frac{1}{n}\left(\frac{I_{\mathrm{calc}}(Q_i) - I_{\mathrm{exp}}(Q_i)}{I_{\mathrm{exp}}(Q_i)}\right)^2}, \tag{4}$$

where n is the number of data points.

Then, one of the molecules is chosen randomly and moved to another lattice point where a molecule does not exist, and $I_{\mathrm{calc}}(Q)$ and χ are calculated again. If χ becomes smaller than before, the movement is accepted. Otherwise, the movement is also accepted with some probability which is proportional to $\exp(-\Delta\chi)$, where $\Delta\chi$ is the difference in χ between before and after moving, in order to avoid falling into a local minimum. This process is iterated 10 million times and finally the χ becomes less than 0.05.

4.2. Results of the RMC analysis

Solid curves in figure 2 show the calculated scattering intensities obtained by the newly developed RMC method. It can be confirmed that the RMC results excellently reproduce the observed SANS intensities for all states. If the computational domain did not have enough size, the oscillation would be imposed on the scattering curves because of the termination error in the Fourier transformation. Since there are no such oscillations in all calculated results as shown in figure 2, the size of computational domain is considered to be sufficient.

Figures 5(a)–(e) display the obtained molecular distribution of CO_2 with the thickness of $2a$ in each state. These images are reasonable structural candidates. The density fluctuation of the molecules can be clearly seen in figure 5 at all thermodynamic states.

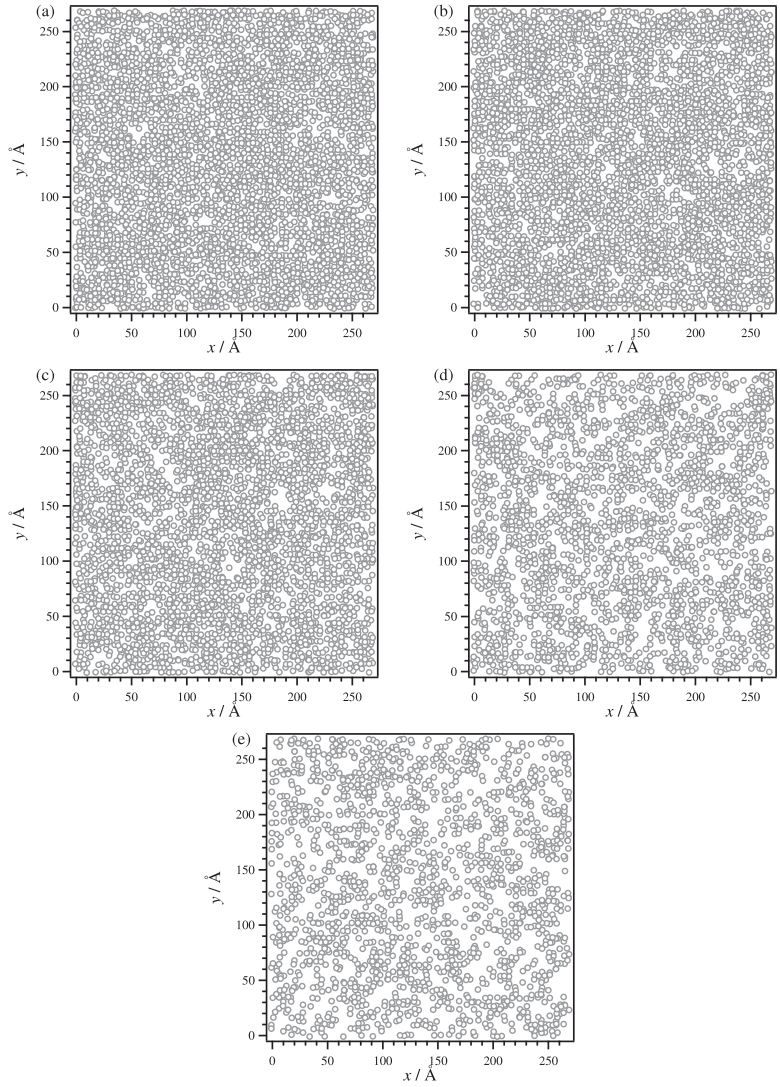

Figure 5. Distribution of CO_2 molecules at a certain plane with the thickness of $2a$ in the computational domain. Panels (a)–(e) display states 1–5 (table 1), respectively.

The pair distribution functions, $g(r)$, calculated from the molecular distribution are shown in figure 6. Although all $g(r)$s have an oscillation with the period of ∼3.4 Å, it is only an artificial one coming from the grids of the structural model. Therefore, the smoothed $g(r)$ over the large region is also drawn in figure 6(b). As shown in figure 6(a), it can be significantly confirmed that $g(r)$ in the short r region ($r < 10$ Å) monotonically decreases with increasing density of the system (from state 5 to state 1). This change indicates that the intermolecular correlation in the short range becomes smaller. On the other hand, $g(r)$ at state 3 has a long tail in the long r region as shown in figure 6(b). This agrees with the correlation length having its maximum at state 3 (figure 4).

5. Discussion

5.1. Approximations in the RMC calculation

It is desirable to describe the validity of our RMC calculation before discussing the main task of assessing structural change along the isotherm. In the RMC calculation, we have applied two artificial approximations in order to shorten the calculating time: one was neglecting the molecular shape by using the isotropic form factor of a CO_2 molecule, and the other was making grids in the computational domain. Here, we discuss the validity of these approximations.

Strongly orientational correlation between CO_2 molecules was reported in the previous studies with wide-angle scattering and molecular dynamics simulation [8–11]. These results suggest that the molecular shape should be taken into account when we construct the structural model in a local region with high spatial resolution. However, in this study, we focus only on the large scale structure with low spatial resolution and the Q range used in our RMC analysis (0.01 Å $< Q <$ 0.5 Å) is far smaller than the peak position of intermolecular correlation, $Q \approx 1.85$ Å^{-1}. Therefore, the effect of molecular shape can be ignored in our RMC calculations.

The grid makes an oscillation in the calculated $g(r)$ as described in the previous section. Nevertheless, the period of oscillation is almost the same as the characteristic length of a

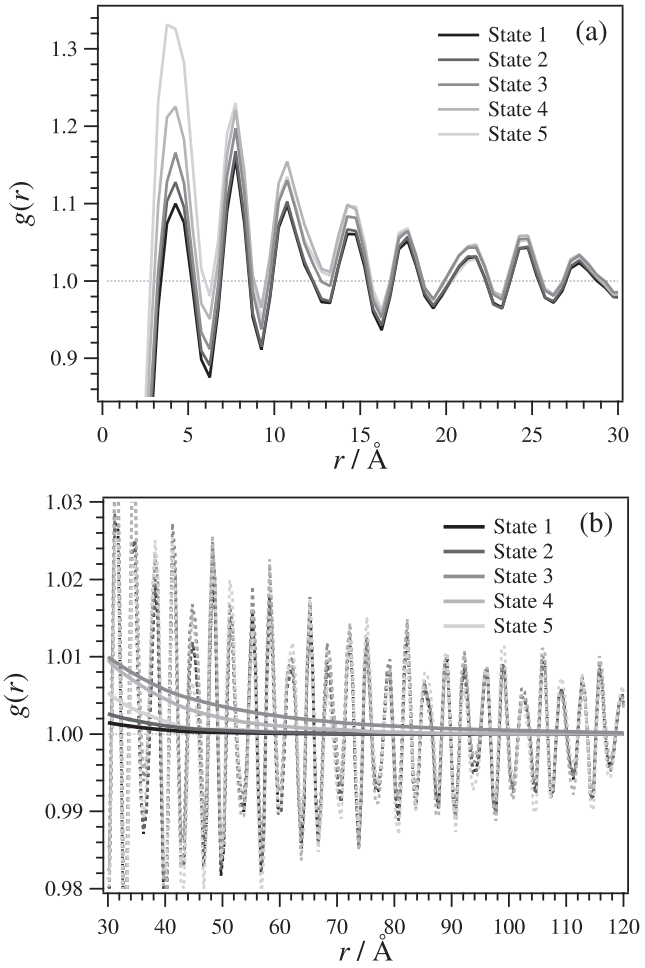

Figure 6. Pair distribution functions, $g(r)$, of the CO_2 molecules calculated by the RMC approach. Short and long range correlations are shown in (a) and (b), respectively. Solid lines in panel (b) show smoothing results.

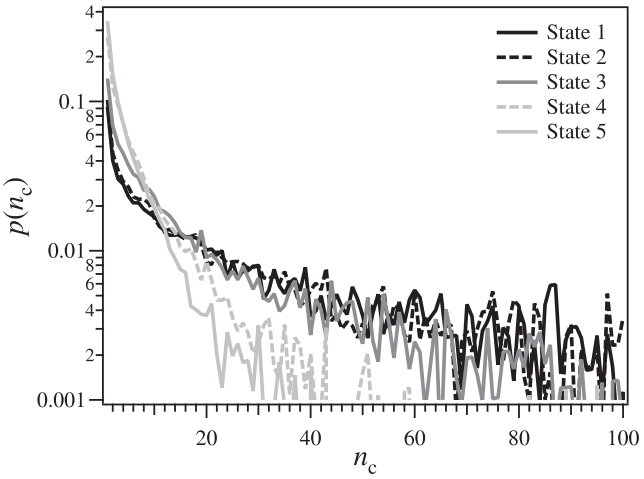

Figure 7. Probability of a molecule belonging to the cluster of size n_c.

CO_2 molecule, a (=3.39 Å), and the Fourier transformation of this oscillation with equation (3) makes only a sharp peak at $Q = 1.85$ Å^{-1} ($=2\pi/a$). Therefore, the grid does not have any effect on the calculated scattering intensity in the Q range from 0.01 to 0.5 Å^{-1}. From the above discussion, we can conclude that these approximations are appropriate.

5.2. Structural change over the ridge

As shown in figure 4, the correlation length along the isotherm has a maximum. The previous study proposed that this behaviour of the correlation length around the ridge could be caused by the change of the observed object: the correlation length indicates the size of clusters in the low density phase (left-hand side of the ridge in figure 4) while it shows the size of voids in the high density phase (right-hand side of the ridge in figure 4) [1]. However, there is room for argument on this point because the definitions of the clusters and the voids are ambiguous. In addition, the correlation length is just the statistical scale of fluctuation and does not directly correspond to the size of cluster or that of the void. To investigate the structural change precisely, the actual size of cluster should be clarified. Therefore, we calculated it with the molecular distribution which was derived from the new RMC method.

Firstly, a cluster is defined in the same way as in percolation analysis: molecules located at the grids of the nearest neighbours are assumed to be involved in the same cluster [19]. Then, a probability function $p(n_c)$ was calculated: $p(n_c)$ indicates the probability that a molecule belongs to a cluster with the number of molecules n_c. The $p(n_c)$s obtained are shown in figure 7. The $p(n_c)$s at states 4 and 5 are higher than those at states 1–3 for $n_c < 10$ while they are quite a bit smaller for $n_c > 10$. This indicates that many small clusters and a few large clusters exist in states 4 and 5, and the ratios of large clusters get higher with increasing density. As an index for this transition, the probability in the cluster for $n_c > 10$, p_L is defined as

$$p_L = \sum_{n_c=11}^{\infty} p(n_c) = 1 - \sum_{n_c=1}^{10} p(n_c), \tag{5}$$

and the density dependence of p_L is displayed in figure 8. p_L shows a monotonic increase with increasing density of states even though the correlation length becomes maximum at state 3. From this result, it can be clearly confirmed that the correlation length does not directly correspond to the actual size of clusters and the change of fluctuation along the isotherm cannot be explained by just the evolution of the size of the clusters.

In order to explain the change of correlation length along the isotherm, the pair distribution function should be focused on. In the first place, we looked at $g(r)$ for state 5 where the density is the lowest of those for all observed states. As shown in figure 6(a), $g(r)$ becomes largest in the short r region ($r <$ 10 Å). This means that the deviation of the local density from the averaged one is larger than for any other states. At the same time, $g(r)$ rapidly converges toward unity, indicating the short correlation length as shown in figure 6(b). In this state, the generation of clusters induces a significant density deviation because the average density is fairly low. This is the reason for

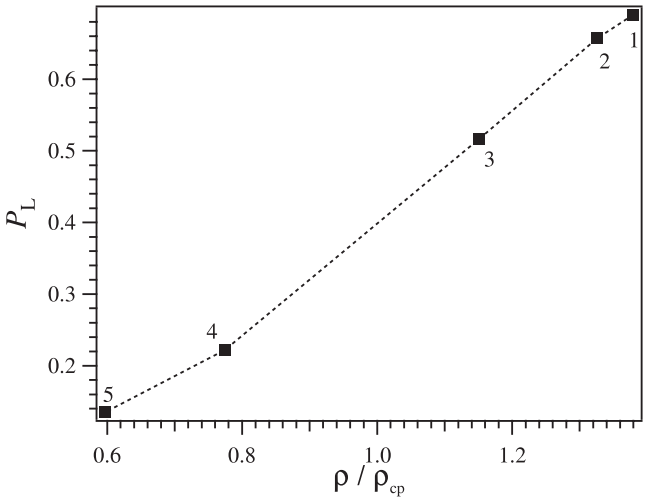

Figure 8. Density dependence of the probability of a molecule belonging to the cluster of size $n_c > 10$. The numbers in the figure denote the state.

the largest $g(r)$ being in the short r region. On the other hand, the short convergence distance can be considered to reflect in the *small* size of cluster, which is shown in figure 7. As a result, the correlation length in this state almost corresponds to the size of clusters.

Next, from state 4 to state 3, $g(r)$ in the short r region becomes smaller while the convergence distance gets longer. The increase of the average density makes the deviation of the local density indistinct. Therefore, $g(r)$ for the small r region becomes smaller in these states. On the other hand, the elongation of the convergence distance comes from the growth of cluster size as shown in figures 7 and 8. Accordingly, it can be said that in these states the growth of the cluster lengthens the correlation length even though the increase of the average density makes the cluster indistinct.

Finally, at states 1 and 2, $g(r)$ for the short r region continuously becomes smaller with increasing density while the distance of convergence becomes shorter than for state 3. In these states, the molecular clusters will submerge in the average density level, which becomes fairly high. As a result of this submergence, the correlation length seems to decrease.

From the above consideration, the structural change along the isotherm (from state 5 to state 1) is suggested to come from two different factors; one is the growth of the cluster size and the other is the increase of the average density. The growth of the cluster enhances the density fluctuation and elongates the correlation length, while the increase of the average density weakens the fluctuation and shortens the correlation length. In the low density phase, the density fluctuation becomes larger with increasing density because the effect of the growth of clusters is dominant. On the other hand, the fluctuation is weakened in the higher density phase because of the increase of the average density. Therefore, the structural change along the isotherm is considered to be caused by the change of balance between the growth of clusters and the increase of the average density.

6. Conclusion

A SANS experiment for sc-CO_2 was carried out along the isotherm near the critical point. The correlation lengths obtained indicate well the ridge in the supercritical region. Moreover, the distributions of molecules over a large domain could be derived from the observed SANS intensities with a newly developed RMC method. The size of clusters calculated with the RMC results shows monotonic increase with increasing density even though the correlation length becomes maximum at the ridge. The pair distribution function, $g(r)$, for $r < 10$ Å, which was also obtained by the RMC calculation, decreases with increasing density of the system, while the convergence distance of $g(r)$ becomes longest at the ridge. It can be suggested from the evolution of the cluster size and $g(r)$ that the structural change along the ridge is caused by the change of balance between the growth of clusters and the increase of the average density.

Acknowledgments

This work was partially supported by a Grant-in-Aid for Creative Scientific Research (No. 16GS0417) and also supported by the New Energy and Industrial Technology Development Organization (NEDO) under the 'Advanced Fundamental Research Project on Hydrogen Storage Materials'. MS is supported by a Grant-in-Aid for Scientific Research of the Ministry of Education, Science and Culture, Japan (No 19540427).

References

[1] Nishikawa K and Tanaka I 1995 *Chem. Phys. Lett.* **244** 149
[2] Nishikawa K, Tanaka I and Amemiya Y 1996 *J. Phys. Chem.* **100** 418
[3] Nishikawa K, Kusano K, Arai A A and Morita T 2003 *J. Chem. Phys.* **118** 1341
[4] Nishikawa K, Arai A A and Morita T 2003 *J. Supercrit. Fluids* **30** 249
[5] Morta T, Nishikawa K, Takematsu M, Iida H and Furutaka S 1997 *J. Phys. Chem.* B **101** 7158
[6] Ishii R, Okazaki S, Okada I, Furusaka M, Watanabe N, Misawa M and Fukunaga T 1995 *Chem. Phys. Lett.* **240** 84
[7] Ishii R, Okazaki S, Odawara O, Okada I, Misawa M and Fukunaga T 1995 *Fluid Phase Equilib.* **104** 291
[8] Ishii R, Okazaki S, Okada I, Furusaka M, Watanabe M, Misawa M and Fukunaga T 1996 *J. Chem. Phys.* **105** 7011
[9] Chiappini S, Nardone M, Ricci F P and Bellissent-Funel M C 1996 *Mol. Phys.* **89** 975
[10] Saharay M and Balasubramanian S 2004 *J. Chem. Phys.* **120** 9694
[11] Zhang Z and Duan Z 2005 *J. Chem. Phys.* **2005** 214507
[12] McGreevy R L and Pusztai L 1988 *Mol. Simul.* **1** 359
[13] Misawa M 2002 *J. Chem. Phys.* **116** 8463
[14] Otomo T, Furusaka M, Satoh S, Itoh S, Adachi T, Shimizu S and Takeda M 1999 *J. Phys. Chem. Solids* **60** 1579
[15] Sugiyama M, Hara K, Hino M, Annaka M, Saito T and Fukunaga T 2003 *Trans. Mater Res. Soc. Japan* **28** 1013
[16] Young D A and Alder B J 1971 *Phys. Rev.* A **3** 364
[17] Misawa M 1990 *J. Chem. Phys.* **93** 8401
[18] Span R and Wagner W 1996 *J. Phys. Chem. Ref. Data* **25** 1509
[19] Stauffer D and Aharony A 1994 *Introduction to Percolation Theory* (London: Taylor and Francis)